

## Importance of Tryptophan 49 of Antithrombin in Heparin Binding and Conformational Activation<sup>†</sup>

Bernhard H. Monien,<sup>‡</sup> Chandravel Krishnasamy,<sup>‡</sup> Steven T. Olson,<sup>§</sup> and Umesh R. Desai<sup>\*‡</sup>

Department of Medicinal Chemistry and Institute for Structural Biology and Drug Discovery,  
Virginia Commonwealth University, Richmond, Virginia 23298-0540, Center for Molecular Biology of Oral Diseases,  
College of Dentistry, University of Illinois at Chicago, Chicago, Illinois 60612

Received April 22, 2005; Revised Manuscript Received June 23, 2005

**ABSTRACT:** Tryptophan 49 of antithrombin, the primary inhibitor of blood clotting proteinases, has previously been implicated in binding the allosteric activator, heparin, by chemical modification and mutagenesis studies. However, the X-ray cocrystal structure of the antithrombin–pentasaccharide complex shows that Trp49 does not contact the bound saccharide. Here, we provide a detailed thermodynamic and kinetic characterization of heparin binding to a Trp49 to Lys variant of antithrombin and suggest a model for how Trp49 participates in heparin binding and activation. Mutation of Trp49 to Lys resulted in substantial losses of 16–24% in heparin-binding energy at pH 7.4, *I* 0.15, and 25 °C. These losses were due to both the loss of one ionic interaction (~30%) and the loss of nonionic interactions (~70%). Rapid kinetics analyses showed that the mutation minimally affected the initial weak binding of heparin to antithrombin or the rate constant for the subsequent conformational activation of the serpin. Rather, the principal effect of the mutation was to increase the rate constant for reversal of the conformational activation step by 70–100-fold, thereby destabilizing the activated conformation. This destabilization could be accounted for by the disruption of a network of interactions involving Trp49, Glu50, and Lys53 of helix A and Ser112 of helix P, which stabilizes the activated conformation.

Antithrombin, a plasma glycoprotein and a member of the serpin superfamily of proteins, is a major inhibitor of several proteinases, especially thrombin and factor Xa, which play pivotal roles in the blood-clotting process (1, 2). Antithrombin inhibits these enzymes using the “suicide substrate”-like serpin inhibition mechanism that results in the formation of a stoichiometric, covalent inhibitor–enzyme complex (3). However, antithrombin inhibition of procoagulant proteinases is extremely slow under physiological conditions with second-order rate constants approaching at most  $10^4 \text{ M}^{-1} \text{ s}^{-1}$  (4–6).

Antithrombin’s physiologically insignificant rate of proteinase inhibition is greatly enhanced by heparin, a naturally occurring, highly sulfated, linear, 1→4-linked copolymer of uronic acid and glucosamine residues (7, 8). The acceleration brought about by polymeric heparin reaches ~600–2000-fold for factor Xa and ~1000–4000-fold for thrombin (5, 6). This acceleration is brought about through two distinct mechanisms, a conformational change mechanism for factor Xa and an approximation mechanism for thrombin. In the

conformational change mechanism, the binding of a specific pentasaccharide sequence in heparin to antithrombin triggers a conformational change in the inhibitor that alters the serpin core structure, including the reactive center loop (RCL)<sup>1</sup> containing the reactive bond, resulting in exposure of exosites, which greatly enhance its ability to recognize factor Xa (9, 10). Unlike factor Xa, the acceleration in inhibition of thrombin is almost exclusively promoted by the formation of a ternary complex between heparin, the inhibitor, and the enzyme, wherein the polysaccharide acts as a bridge on which thrombin and antithrombin meet (11–13). In this approximation mechanism, the conformational change induced in antithrombin serves to primarily afford a high-affinity binding site to heparin and minimally to enhance the rate of the inhibition reaction. A similar mechanism also plays an important role in factor Xa inhibition in the presence of physiologic levels of calcium ions (14, 15).

Major efforts have been directed to identify amino acids that influence antithrombin binding to heparin and activation of the inhibitor. The X-ray crystal structure of antithrombin in complex with a high-affinity heparin pentasaccharide reveals a number of positively charged residues in the heparin-binding site (16). These include Lys11, Arg13,

<sup>†</sup> This work was supported by the American Heart Association, Chicago affiliate (to U.R.D.), the American Heart Association, Mid-Atlantic affiliate (to U.R.D., 0256286U), and the National Heart, Lung, and Blood Institute (to U.R.D., RO1 HL69975, and to S.T.O., RO1 HL 39888).

\* To whom correspondence should be addressed: Department of Medicinal Chemistry, Virginia Commonwealth University, 410 N. 12th Street, P.O. Box 980540, Richmond, VA 23298-0540. Telephone: 804-828-7328. Fax: 804-827-3664. E-mail: urdesai@vcu.edu.

<sup>‡</sup> Virginia Commonwealth University.

<sup>§</sup> University of Illinois at Chicago.

<sup>1</sup> Abbreviations: AT, antithrombin; BHK, baby hamster kidney; DEFGH, heparin pentasaccharide DEFGH;  $\Delta G^\circ$ , standard free energy of binding;  $\Delta G^\circ_{\text{ionic}}$ , standard free energy of binding because of ionic interactions only;  $\Delta G^\circ_{\text{nonionic}}$ , standard free energy of binding because of nonionic interactions only; H, heparin; HAH, high-affinity heparin;  $K_d$ , equilibrium dissociation constant;  $K_{d,\text{nonionic}}$ , equilibrium dissociation constant associated with nonionic interactions only; PEG, poly(ethylene glycol); RCL, reactive center loop; Wt, wild-type.



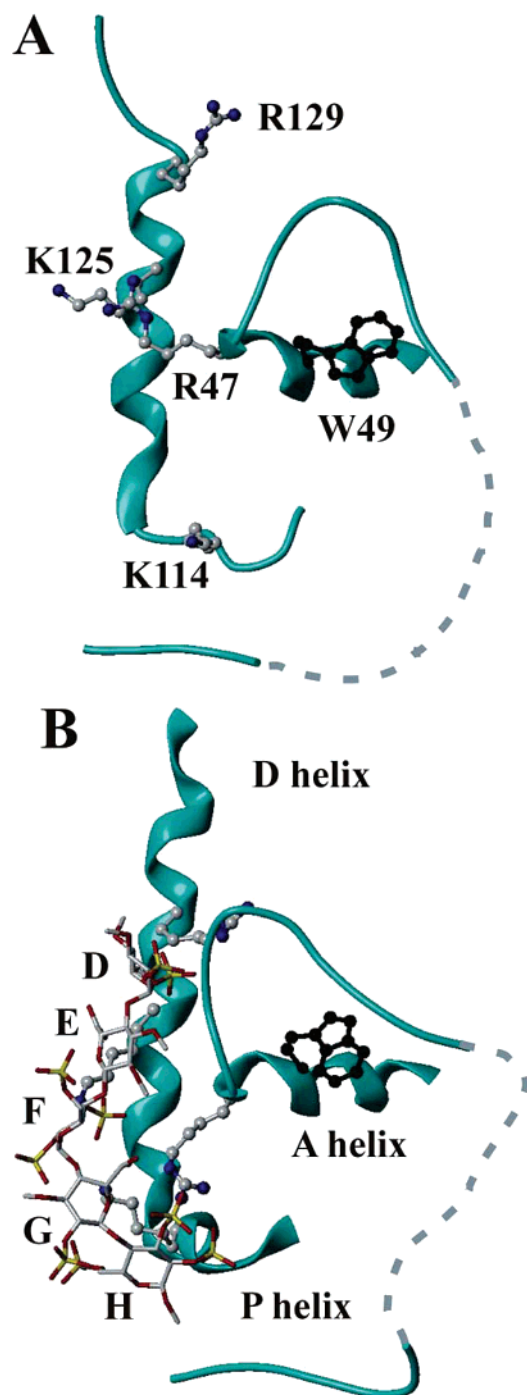


FIGURE 1: Orientation of tryptophan 49 in the native state (A) and allosterically activated state (B) of antithrombin. Shown are the refined structures of free (A) and heparin pentasaccharide-complexed (B) antithrombin taken from PDB files “1E05” and “1E03” (<http://www.rcsb.org/pdb>), respectively. The side chains of important residues of the heparin-binding site, Lys114, Lys125, and Arg129 belonging to helix D, and the N-terminal A helix residues, Arg47 and Trp49, as well as the heparin pentasaccharide (DEFGH), are shown in ball-and-stick representation. The dashed line in both A and B represents the unstructured region of the N-terminal end of the polypeptide chain. For the purpose of this figure, the side chains of Lys125 in 1E03 and Lys114 in 1E05 that are absent in the crystal structure were engineered into the inhibitor and the structure was minimized. Note that Trp49 is oriented away from and does not contact the cofactor, heparin pentasaccharide, in the complex.

Arg24, Arg46, Arg47, Lys114, Lys125, Arg129, Arg132, Lys133, and Arg136. Of these, mutagenesis studies show

that Lys114, Lys125, and Arg129 contribute most of the free energy of binding to the heparin–antithrombin interaction (Figure 1) (17–20) and more importantly constitute the core of a network of cooperative interactions.

Detailed biochemical studies show that, although the heparin–antithrombin interaction appears to be primarily electrostatic, a significant component, ~60%, of the binding energy arises from nonionic forces (21). Several nonionic residues, including Pro41, Trp49, Leu99, Ser116, and Gln118, present near the binding site are known to introduce a heparin-binding defect when mutated (22–27). Tryptophan 49 was one of the first residues suggested to play an important role in heparin binding to antithrombin based on the effects of chemical modification of this residue (23, 24). Subsequent studies of a recombinant Trp49Lys antithrombin variant showed that Trp49 contributed 8–18% to the total binding energy, from which it was concluded that Trp49 was a heparin contact residue (28). However, the X-ray crystal structure of the antithrombin–pentasaccharide complex later showed that Trp49 points away from the pentasaccharide (16) and is not in direct contact with the activator (Figure 1). Recent crystal structure of the heparin-bound intermediate state also indicates that Trp49 is not in the vicinity of the pentasaccharide in the initial binding process (29). These studies raise questions on the functional role of Trp49 residue in heparin activation of antithrombin.

We have characterized in detail the thermodynamics and kinetics of heparin binding and activation of Trp49Lys antithrombin to better understand the role of Trp49 in heparin activation of the inhibitor. Our results suggest that Trp49 plays an important role in mediating the conformational changes in the heparin-binding site, which are required for high-affinity heparin binding and antithrombin activation. Mutation of Trp49 thus reduces heparin-binding affinity principally by destabilizing the activated antithrombin conformation. The X-ray structures of free and heparin-bound antithrombin reveal that Trp49 is part of a conformational switch involving Glu50, Lys53, and Ser112, which mediates structural changes in helix A and promotes the formation of helix P. All residues involved in this conformational switch are highly conserved among vertebrate antithrombins (30), consistent with an important role in stabilizing the activated conformation. These findings provide new insights into the mechanism of heparin binding and activation of antithrombin.

## EXPERIMENTAL PROCEDURES

**Proteins and Heparins.** Two recombinant antithrombins, W49K and N135Q, were expressed in baby hamster kidney (BHK) cells as described previously (31, 32). The previously characterized N135Q antithrombin variant served as the wild-type control. The purification essentially followed the protocol developed for plasma antithrombin, which includes heparin-Sepharose affinity and anion-exchange and size-exclusion chromatographies to isolate monomeric forms of the inhibitor variants (4). Whereas the high heparin-affinity glycoform of N135Q antithrombin eluted at ~1.5–1.7 M NaCl, the comparable glycoform of W49K protein eluted at ~0.9 M NaCl concentration. Both N135Q and W49K antithrombin glycoforms lack a carbohydrate chain at the N135 position, thus resembling plasma  $\beta$  antithrombin (33). Protein concentrations were determined spectrophotometrically using  $A^{1\%}_{280} = 6.5$  for N135Q and a calculated  $A^{1\%}_{280}$



of 5.5 for W49K antithrombin based on the loss of one tryptophan out of four in the protein. Full-length heparin with a high affinity for antithrombin and with a highly reduced polydispersity and average molecular mass of 8000 Da (~26 saccharide units) was isolated from commercial heparin by size and affinity fractionation as described previously (4, 21, 34). The synthetic antithrombin-binding pentasaccharide, DEFGH, was generously provided by Maurice Petitou (Sanofi Recherche, Toulouse, France).

**Stoichiometry of Inhibition (SI).** The stoichiometry of antithrombin inhibition of thrombin was measured as previously described to ascertain the proportion of active inhibitor in the recombinant antithrombin preparations (4). Briefly, recombinant antithrombin was added to identical samples of thrombin (10–200 nM) to give molar ratios of inhibitor/proteinase ranging from 0 to 5. After incubation for 5–18 h, residual thrombin activity was determined spectrophotometrically from the initial rate of hydrolysis of 100  $\mu$ M S-2238 substrate (Chromogenix, Franklin, OH) in 1, 0.15 buffer and pH 7.4. Linear regression fitting of the residual thrombin activities as a function of the molar ratio of the inhibitor/enzyme yielded the SI from the abscissa intercept (4). SI values ranged from 1.2 to 1.8 and 1.2 to 1.9 for the N135Q and W49K mutants, respectively. Typically, higher activity preparations with SI values closer to 1 were used for equilibrium binding titrations. SI values greater than 1 were accounted for by the presence of the inactive latent form in both recombinant proteins, as judged by SDS–PAGE, and not because of an intrinsic loss of inhibitory function. SI values were used to calculate the concentration of active inhibitor for kinetic analyses of factor Xa and thrombin inhibition. For the W49K mutant, the SI values correlated well with the stoichiometry of heparin binding as determined in fluorescence titrations performed at inhibitor concentrations much greater than the  $K_d$  for the interaction (see below) (4).

**Experimental Conditions.** Experiments were performed at 25 °C in 20 mM sodium phosphate buffer, adjusted to either pH 6.0 or 7.4, containing 0.1 mM EDTA and 0.1% (w/v) PEG8000. NaCl was added to achieve higher ionic strengths. The ionic strength of the buffer under these conditions in the absence of any added salt was 0.025 (pH 6.0) and 0.05 (pH 7.4).

**Equilibrium Binding Titrations.** Dissociation constants ( $K_d$ ) for the interaction between antithrombin mutants, N135Q and W49K, and full-length heparin as well as heparin pentasaccharide were determined by direct equilibrium binding measurements at 25 °C and pH 7.4 or 6.0. Antithrombin variants were titrated with solutions of the saccharides up to a saturation of 80–95% using the increase in intrinsic protein fluorescence at 340 nm on a SLM 8000C spectrofluorometer (SLM Instruments, Rochester, NY). Titrations were performed in duplicate. The recorded changes in fluorescence in heparin-binding titrations were fitted to the quadratic equilibrium binding equation using a 1:1 binding stoichiometry as previously described (4, 21).

To resolve the ionic and nonionic contributions to the total binding energy, titrations were performed in buffers of different ionic strengths, as described earlier (21, 32). Briefly, the contributions were obtained using the linear dependence of the logarithm of the observed dissociation constant ( $K_{d,obs}$ ) on the logarithm of  $[Na^+]$  according to the equation  $\log K_{d,obs} = \log K_{d,nonionic} + Z\psi \log [Na^+]$ , where  $K_{d,nonionic}$  is the salt-

independent dissociation constant,  $Z$  is the total number of charge–charge interactions involved in the association of the protein with heparin, and  $\psi$  is the fraction of monovalent counterions bound per heparin ionic charge that are released upon protein binding (21, 35, 36). Least-squares regression analysis yielded the nonionic component of the binding energy from the intercept,  $\log K_{d,nonionic}$ , and the value of  $Z$  from the slope after dividing by the value of 0.8 for  $\psi$  (35).

**Stopped-Flow Kinetics of Heparin Binding.** The kinetics of high-affinity heparin and pentasaccharide binding to variant N135Q antithrombin and W49K antithrombin were analyzed at 25 °C, pH 7.4, and  $I$  0.15 in an SX-17MV stopped-flow apparatus (Applied Photophysics, Leatherhead, U.K.), essentially as described earlier (21, 37). Binding was followed by the increase of tryptophan fluorescence emission using an emission cutoff filter at 310 nm ( $\lambda_{ex} = 280$  nm). Pseudo-first-order conditions were achieved by employing at least a 10-fold molar ratio of heparin (or pentasaccharide) to antithrombin. Nonlinear regression fitting of the progress curves with a single-exponential function yielded the observed pseudo-first-order rate constant,  $k_{obs}$ , measured at various concentrations of heparin or pentasaccharide. For each set of concentrations, approximately 10 reaction traces were collected for about 3–5 half-lives and averaged.

**Kinetics of Proteinase Inactivation.** Second-order rate constants for inhibition of proteinases by the antithrombin variants N135Q and W49K alone as well as in the presence of high-affinity heparin and pentasaccharide were determined under pseudo-first-order conditions with catalytic amounts of saccharides at 25 °C; pH 7.4, and  $I$  0.15, as previously described (4). Reaction solutions of 100  $\mu$ L containing 25–100 nM antithrombin, 0–5 nM heparin, and 5–20 nM protease were quenched by adding 100  $\mu$ M S-2238 or 100–200  $\mu$ M Spectrozyme FXa (American Diagnostica, Greenwich, CT) for thrombin and factor Xa, respectively. The residual enzymatic activity, monitored at various time intervals, was obtained spectrophotometrically ( $\lambda_{max} = 405$  nm) from the initial rate of substrate cleavage. The decrease in residual enzyme activity as a function of time was fitted to a single-exponential equation to give the pseudo-first-order rate constant ( $k_{obs}$ ) of proteinase inhibition. Second order-rate constants,  $k_{uncat}$ , for the reactions between proteinases and antithrombin variants alone were calculated from the ratio of  $k_{obs}$ /antithrombin concentration. In the presence of saccharides, the second-order rate constants for the uncatalyzed and catalyzed protease inhibition,  $k_{uncat}$  and  $k_{act}$ , respectively, were determined from the intercept of the  $y$  axis ( $k_{uncat}$ ) and the slope ( $k_{act}$ ) of the plot of  $k_{obs}$  versus the saccharide concentration according to eq 1

$$k_{obs} = k_{uncat}[AT]_o + k_{act} \frac{[AT]_o[H]_o}{[AT]_o + K_d} \quad (1)$$

where  $[AT]_o$  and  $[H]_o$  are the initial concentrations of antithrombin variants and heparin (or pentasaccharide), respectively, and  $K_d$  is the observed equilibrium dissociation constant of the antithrombin–heparin interaction.

## RESULTS

**Affinity of Heparin Binding by Fluorescence Titrations.** Fluorescence titrations of high-affinity heparin and pentasaccharide binding to antithrombin mutants N135Q and W49K



Table 1: Equilibrium Dissociation Constants ( $K_d$ ), Maximal Fluorescence Enhancements ( $\Delta F_{\max}$ ), and Heparin-Independent and -Dependent Factor Xa and Thrombin Inhibition Rate Constants ( $k_{\text{uncat}}$  and  $k_{\text{act}}$ ) for the Interaction of Full-Length Heparin (HAH) and Heparin Pentasaccharide (H5) with W49K and Control Recombinant Antithrombins<sup>a</sup>

heparin	AT	condition	$K_d$ (nM)	$\Delta F_{\max}$ (%)	$k_{\text{uncat}}$		$k_{\text{act}}$		acceleration
					factor Xa (mM <sup>-1</sup> s <sup>-1</sup> )	thrombin (mM <sup>-1</sup> s <sup>-1</sup> )	factor Xa (mM <sup>-1</sup> s <sup>-1</sup> )	thrombin [10 <sup>3</sup> × (mM <sup>-1</sup> s <sup>-1</sup> )]	$k_{\text{act}}/k_{\text{uncat}}$
HAH	W49K	pH 7.4, <i>I</i> 0.15	21 ± 4	36 ± 4		9.8 ± 0.8		18.0 ± 1.0	1840 ± 180
HAH	N135Q	pH 7.4, <i>I</i> 0.15	0.7 ± 0.1 <sup>b</sup>	40 ± 4		9.2 ± 0.4 <sup>c</sup>		13.0 ± 1.0 <sup>c</sup>	1413 ± 170
H5	W49K	pH 7.4, <i>I</i> 0.15	257 ± 44	31 ± 4	5.9 ± 0.5		900 ± 270		152 ± 58
H5	N135Q	pH 7.4, <i>I</i> 0.15	2.0 ± 0.2 <sup>d</sup>	35 ± 2	4.5 ± 0.1 <sup>c</sup>		460 ± 60 <sup>c</sup>		102 ± 16
H5	W49K	pH 6.0, <i>I</i> 0.02	17 ± 5	26 ± 2					
H5	N135Q	pH 6.0, <i>I</i> 0.02	~4 × 10 <sup>-6</sup> <sup>d</sup>	31 ± 3					

<sup>a</sup> See the Experimental Procedures for a description of how these parameters were determined. All errors represent ±1 SE. <sup>b</sup> Calculated from the salt dependence of  $K_{d,\text{obs}}$  for the HAH–N135Q antithrombin interaction, which was found to have a slope of  $4.3 \pm 0.2$  and an intercept of  $-5.4 \pm 0.1$ . <sup>c</sup> Taken from Chuang, Y.-J., Gettins, P. G. W., and Olson, S. T. (1999) *J. Biol. Chem.* 274, 28142–28149. <sup>d</sup> Calculated from the salt dependence of  $K_{d,\text{obs}}$  for the H5–N135Q antithrombin interaction (see Table 2).

were performed as previously done with other antithrombin mutants. The binding of heparin (or pentasaccharide) gives rise to an overall increase in intrinsic tryptophan fluorescence of approximately 30–40%, resulting from changes in the environment of all four Trp residues, W49, W189, W225, and W307, caused by conformational activation (31). This increase is saturable and can be fit to a quadratic binding equation to yield the equilibrium dissociation constant  $K_d$  of the interaction (4).

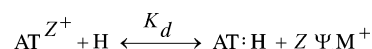
Table 1 summarizes the binding affinity and maximal fluorescence changes observed at pH 7.4 and 6.0. Whereas the N135Q wild-type antithrombin control showed 31–40% increases in fluorescence, the W49K variant antithrombin showed 26–36% increases (Figure 2). The contribution of W49 to the intrinsic tryptophan fluorescence of wild-type antithrombin is 8 and 12% in the unactivated and heparin-activated states, respectively (31). On the basis of these contributions, it can be predicted that the fluorescence enhancement accompanying heparin binding to W49K antithrombin will decrease to 85% of that of the wild-type inhibitor. Our results therefore suggest that heparin induces a normal fluorescence enhancement in W49K antithrombin.

Equilibrium dissociation constants ( $K_d$ ) for full-length heparin and pentasaccharide interacting with W49K anti-

thrombin at pH 7.4 were found to be 21 and 257 nM, respectively (Table 1). The corresponding  $K_d$  values for these saccharides interacting with the reference, N135Q, antithrombin were 0.7 and 2 nM, which were calculated from salt dependence studies (see below and the caption of Table 1). Replacement of Trp49 with Lys, thus, results in a 30-fold weakening of antithrombin-binding affinity for full-length heparin and a 130-fold weakening of the affinity for pentasaccharide, corresponding to standard free energy of binding defects ( $\Delta\Delta G^\circ = -RT \ln(K_{d,\text{W49K}}/K_{d,\text{N135Q}})$ ) of 2.0 and 2.9 kcal/mol, respectively.

**Ionic Strength Dependence of Pentasaccharide Binding.** The binding of the heparin pentasaccharide to antithrombin involves an ion-exchange process (Scheme 1), in which the for-

Scheme 1



mation of Z electrostatic interactions is accompanied by a displacement of  $\Psi \text{M}^+$  counterions from the polyelectrolyte (38)

$$\log K_{d,\text{obs}} = \log K_{d,\text{nonionic}} + Z\Psi \log [\text{Na}^+] \quad (2)$$

Here,  $\Psi$  is the effective fraction of counterions  $\text{M}^+$  bound to the pentasaccharide molecule per negative charge, which has been calculated to be 0.8 from the linear charge density of heparin (34). Thus, the observed equilibrium constant ( $K_{d,\text{obs}}$ ) is highly dependent on the ionic strength of the medium and can be described by the linear eq 2 (38), wherein  $K_{d,\text{nonionic}}$  is the nonionic contribution to the overall binding affinity. Therefore, the slope of a double logarithmic plot of  $K_{d,\text{obs}}$  versus  $[\text{Na}^+]$  provides the number of salt bridges (Z) formed in the interaction, and the intercept on the ordinate axis yields  $K_{d,\text{nonionic}}$ .

To determine the effect of the W49K mutation on the ionic and nonionic interactions involved in pentasaccharide binding, the dissociation constant ( $K_{d,\text{obs}}$ ) for pentasaccharide binding to W49K antithrombin was measured as a function of the ionic strength of the buffer. Figure 3 shows the graph of  $\log K_{d,\text{obs}}$  versus  $\log [\text{Na}^+]$  at pH 7.4 and 6.0. Linear regression fits of the data gave Z and  $\log K_{d,\text{nonionic}}$  values of  $4.0 \pm 0.2$  and  $-3.8 \pm 0.2$  at pH 7.4 and  $5.9 \pm 0.6$  and  $-3.8 \pm 0.2$  at pH 6.0 for the W49K–pentasaccharide interaction. The corresponding Z and  $\log K_{d,\text{nonionic}}$  values for N135Q were  $5.0 \pm 0.1$  and  $-5.2 \pm 0.0$  at pH 7.4 and  $5.8 \pm 0.4$  and  $-5.9 \pm 0.1$ , respectively, at pH 6.0. These data indicate that ~4

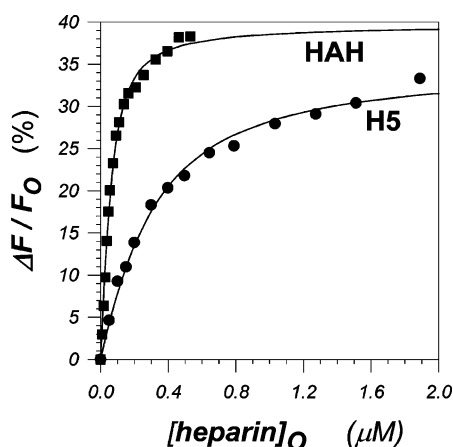


FIGURE 2: Fluorescence titrations of Trp49Lys antithrombin with high-affinity heparin (HAH, ■) and pentasaccharide (H5, ●) at pH 7.4, *I* 0.15; and 25 °C. Titrations were performed as described in the experimental part, and fluorescence changes were fit to the quadratic binding equation assuming a 1:1 interaction (—) to obtain the equilibrium dissociation constant for the antithrombin–cofactor interaction ( $K_{d,\text{obs}}$ ) and maximum fluorescence change ( $\Delta F_{\max}$ ).



Table 2: Ionic and Nonionic Interaction Parameters for W49K and Wild-Type N135Q Antithrombins Interacting with Heparin Pentasaccharide<sup>a</sup>

	pH	Z	$K_{d,nonionic}$ ( $\mu$ M)	$\Delta G_{ionic}^\circ$ (kcal/mol)	$\Delta G_{nonionic}^\circ$ (kcal/mol)
W49K	7.4	$4.0 \pm 0.2$	$158 \pm 27$	-3.8	-5.2
N135Q	7.4	$5.0 \pm 0.1$	$6.3 \pm 0.3$	-4.8	-7.1
W49K	6.0	$5.9 \pm 0.6$	$158 \pm 27$	-5.6	-5.2
N135Q	6.0	$5.8 \pm 0.4$	$1.3 \pm 0.1$	-5.5	-8.1

<sup>a</sup> The number of sodium ions released in the overall binding of heparin pentasaccharide to antithrombin,  $Z\Psi$  (eq 2) was obtained from the slopes of double-logarithmic plots of observed dissociation constants (Figure 3) versus the sodium concentration.  $K_{d,nonionic}$  was obtained from the intercepts of these plots. See the Experimental Procedures for details.

and  $\sim 6$  ion-pair interactions contribute to the W49K antithrombin–pentasaccharide interaction at pH 7.4 and 6.0, respectively, while about 5 and 6 ion pairs contribute to the N135Q antithrombin–pentasaccharide interaction at these pH values (Table 2). Thus, the mutation of W49 results in a loss of nearly one charge–charge interaction at pH 7.4, while at pH 6.0, this lost interaction is restored. The loss of an ionic interaction at pH 7.4 contributes 1.0 kcal/mol to the binding energy loss ( $\Delta G_{ionic}^\circ$ ) (Table 2).

The intercepts correspond to a nonionic binding affinity of 158  $\mu$ M for W49K antithrombin at both pH 7.4 and 6.0. In contrast, the  $K_{d,nonionic}$  values were 6.3 and 1.3  $\mu$ M at pH 7.4 and 6.0, respectively, for the reference N135Q antithrombin (Table 2). Thus, the mutation of the W49 residue results in a loss of  $\sim 25$ - and 120-fold in nonionic binding affinity at pH 7.4 and 6.0, respectively. This corresponds to substantial 1.9 and 2.9 kcal/mol reductions in nonionic binding energy ( $\Delta \Delta G_{nonionic}^\circ$ ) at pH 7.4 and 6.0, respectively, for the mutant W49K antithrombin–pentasaccharide interaction relative to the control inhibitor interaction. These losses in nonionic binding energy correspond to 27 and 36% decreases in the total free energy of binding at pH 7.4 and 6.0, respectively, associated with Trp49  $\rightarrow$  Lys mutation.

**Rapid Kinetics of Heparin Binding.** Binding of heparin (or pentasaccharide) to antithrombin has been shown to follow an induced-fit mechanism, wherein a loose encounter complex AT:H is formed first, which converts to a high-affinity complex AT\*:H via a change in the conformation of the inhibitor (Scheme 2) (21, 37).

In Scheme 2,  $K_1$  and  $K_2$  are the equilibrium dissociation constants for the initial recognition step and the subsequent

Scheme 2



conformational change step, respectively. The initial recognition step is a rapid equilibrium step, while the conformational change step can be resolved in an equilibrium involving forward ( $k_2$ ) and reverse ( $k_{-2}$ ) steps. The two-step reaction is evidenced by a hyperbolic dependence of the observed pseudo-first-order rate constant ( $k_{obs}$ ) on the activator concentration as shown in eq 3

$$k_{obs} = \frac{k_2[H]_0}{K_1 + [H]_0} + k_{-2} \quad (3)$$

The dependence of  $k_{obs}$  on the full-length heparin or pentasaccharide concentration for the binding of heparin to W49K and N135Q antithrombins at pH 7.4,  $I$  0.15; and 25  $^\circ$ C (Figure 4) was analyzed using eq 3 to yield the first-

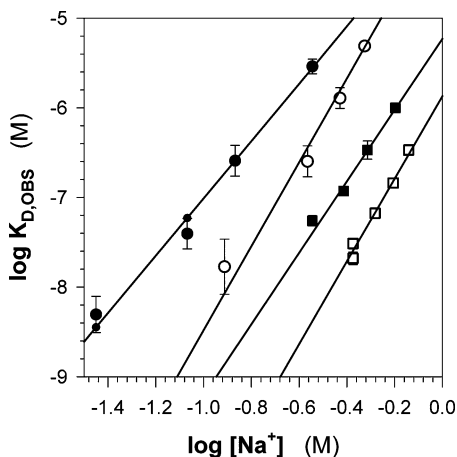


FIGURE 3: Dependence of the equilibrium dissociation constant ( $K_{d,obs}$ ) on the concentration of  $Na^+$  for pentasaccharide DEFGH binding to N135Q ( $\square$  and  $\blacksquare$ ) and W49K ( $\circ$  and  $\bullet$ ) antithrombins at pH 7.4 ( $\blacksquare$  and  $\bullet$ ) and 6.0 ( $\square$  and  $\circ$ ). Solid lines represent the linear regression fits of the data to eq 2. Error bars shown are  $\pm 1$  SE.

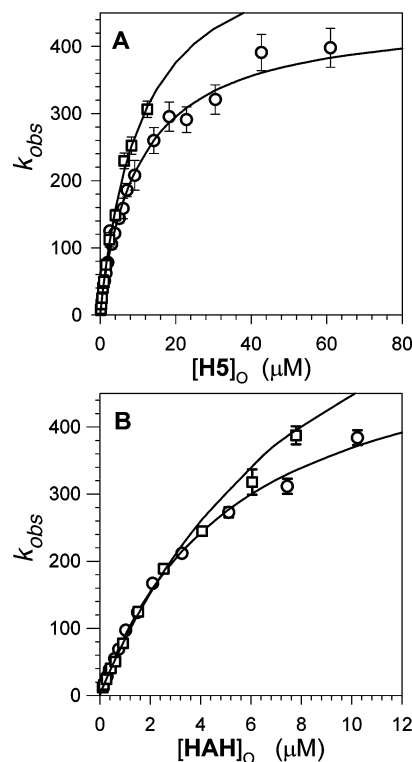


FIGURE 4: Dependence of the pseudo-first-order rate constant  $k_{obs}$  for pentasaccharide (A) and full-length high-affinity heparin (B) binding to the N135Q ( $\square$ ) and W49K antithrombin ( $\circ$ ) at pH 7.4,  $I$  0.15 and 25  $^\circ$ C. Solid lines represent nonlinear regression fits of the data to eq 3 to give the rate constants for the forward ( $k_2$ ) and reverse reaction ( $k_{-2}$ ) of antithrombin conformational activation and the rapid equilibrium dissociation constant for the initial binding step ( $K_1$ ) (Table 3). Error bars shown are  $\pm 1$  SE.



Table 3: Kinetic Constants for W49K and Control Recombinant Antithrombins Interacting with Heparin Pentasaccharide (H5) and Full-Length High-Affinity Heparin (HAH) at pH 7.4, *I* 0.15 and 25 °C<sup>a</sup>

heparin	AT	$K_1$ ( $\mu$ M)	$k_2$ (s <sup>-1</sup> )	$k_{-2}$ (s <sup>-1</sup> )	$K_{d,calcd}$ (nM)	$K_{d,obs}$ (nM)
HAH	W49K	5.4 ± 0.5	565 ± 39	4.3 ± 0.7 <sup>b</sup>	41	21
HAH	N135Q	9.8 ± 0.8	887 ± 56	0.063 <sup>c</sup>	na <sup>d</sup>	
H5	W49K	10.8 ± 2.2	439 ± 33	11.4 ± 0.3 <sup>b</sup>	278	257
H5	N135Q	10.9 ± 1.3	580 ± 47	0.11 <sup>c</sup>	na <sup>d</sup>	

<sup>a</sup> The equilibrium dissociation constant for the first step ( $K_1$ ) and the rate constants for the forward ( $k_2$ ) and reverse ( $k_{-2}$ ) steps were obtained by fitting the data of Figure 4 to eq 3 using nonlinear least-squares analysis. All errors represent ±1 SE. <sup>b</sup> Obtained by using the first five data points of Figure 4 and fitting them to a linear equation  $k_{obs} = k_{on}[H5]_0 + k_{off}$ , where  $k_{off} = k_{-2}$ . <sup>c</sup> Calculated from the equation  $k_{-2} = K_{d,obs}[k_2/K_1]$ . <sup>d</sup> Not applicable.

order rate constants for the forward ( $k_2$ ) and reverse ( $k_{-2}$ ) reactions of the conformational activation step, as well as the equilibrium dissociation constant  $K_1$  for the initial binding step (Table 3). For the control N135Q antithrombin reaction, the reverse reaction rate constant,  $k_{-2}$ , was indistinguishable from 0 and hence was calculated from the relationship  $k_{-2} = K_{d,obs}(k_2/K_1)$ .

The rapid equilibrium dissociation constant  $K_1$  for the recognition step was found to be  $5.4 \pm 0.5$  and  $10.8 \pm 2.2$   $\mu$ M for W49K antithrombin interacting with full-length heparin and pentasaccharide, respectively, while it was  $9.8 \pm 0.8$  and  $10.9 \pm 1.3$   $\mu$ M for N135Q antithrombin reactions with the two respective heparins. Thus, mutation of Trp49 to Lys resulted in no effect on the recognition of the pentasaccharide but a small 1.8-fold enhancement in affinity of the recognition complex for the full-length heparin. The rate constants for the forward conformational activation  $k_2$  were  $565 \pm 39$  and  $439 \pm 33$  s<sup>-1</sup> for W49K interacting with full-length heparin and pentasaccharide, respectively, while the corresponding values for N135Q antithrombin were  $887 \pm 56$  and  $580 \pm 47$  s<sup>-1</sup>. Thus, the rate constants for the forward conformational change in the control N135Q antithrombin reaction are 1.3–1.6-fold better than those observed for the variant W49K antithrombin reaction. Finally, the rate constants for reversal of the conformational change,  $k_{-2}$ , were found to be 4.3 and 11.4 s<sup>-1</sup> for full-length heparin and pentasaccharide binding to W49K antithrombin, respectively, while the values were 0.06 and 0.1 s<sup>-1</sup>, respectively, for the binding of these heparins to N135Q antithrombin (Table 3). Thus, in contrast to  $K_1$  and  $k_2$ , the rate constant for reversal of the conformational change ( $k_{-2}$ ) in W49K antithrombin reactions is ~68- and ~104-fold higher than that in the N135Q antithrombin reactions with full-length heparin and pentasaccharide, respectively. Because  $k_{-2}$  controls the dissociation of heparin from the serpin ( $k_{-2} = k_{off}$ ), these differences account for the majority of binding defects for heparin and pentasaccharide interacting with W49K antithrombin. These data illustrate that replacement of Trp49 with Lys has a dominant effect on the second conformational activation step of the two-step heparin-binding reaction.

**Kinetics of Proteinase Inhibition.** The effect of the W49K mutation on the inhibitory activity of the serpin was determined by measuring the second-order rate constants for antithrombin inhibition of thrombin and factor Xa in the absence and presence of saccharide activators at pH 7.4, as

in previous studies (4). In the absence of a catalyst, second-order inhibition rate constants for W49K antithrombin inhibiting thrombin and factor Xa were measured to be 9800 and 5900 M<sup>-1</sup>s<sup>-1</sup>, which correspond favorably with the values measured for the reference N135Q inhibitor (Table 1). To determine whether heparin activation of antithrombin's inhibitory function is affected by mutation of the W49 residue, second-order rate constants ( $k_{act}$ ) for antithrombin inhibition of thrombin and factor Xa were determined in the presence of the full-length heparin or the pentasaccharide at pH 7.4. The reason for employing different heparins was that heparin accelerates the antithrombin–thrombin reaction by bridging the two proteins in a ternary complex, whereas it accelerates the antithrombin–factor Xa reaction through an allosteric activation of antithrombin brought about by the sequence-specific pentasaccharide. The inhibition rate constants ( $k_{act}$ ) were determined from the slope of the  $k_{obs}$  versus the activator concentration plots, according to eq 1 in Experimental Procedures (Table 1). The full-length heparin accelerated the W49K antithrombin reaction with thrombin  $1840 \pm 180$ -fold relative to the uncatalyzed reaction, in close agreement with the  $1410 \pm 170$ -fold acceleration of the reference N135Q antithrombin–thrombin reaction. The pentasaccharide accelerated the reaction of W49K antithrombin with factor Xa nearly  $152 \pm 58$ -fold relative to the uncatalyzed rate, close to the acceleration of  $102 \pm 16$ -fold achieved for the N135Q antithrombin–factor Xa reaction (Table 1). Thus, the W49K mutation had no significant effects on either the uncatalyzed or heparin-catalyzed reactions of antithrombin with thrombin and factor Xa.

## DISCUSSION

The goal of the present study was to determine how Trp49 of antithrombin contributes to heparin binding and conformational activation of the serpin without directly interacting with heparin. Our studies have confirmed the significant defect in heparin binding produced by mutating Trp49 to Lys in antithrombin, which was shown in a previous study (28). However, our results suggest that the actual binding defect is larger than previously reported. Our studies with a recombinant  $\beta$ -like form of antithrombin lacking carbohydrate at the N135 glycosylation site showed that the Trp49 mutation resulted in a 2.9 kcal/mol loss in pentasaccharide-binding energy and 2.0 kcal/mol loss in full-length heparin-binding energy representing 16–24% of the total binding energy at *I* 0.15, pH 7.4, and 25 °C. This compares with the lower 1.8 and 0.8 kcal/mol binding energy losses for pentasaccharide and full-length heparin interactions with the W49K recombinant antithrombin reported previously under these conditions (28). Because the latter study was done before it was realized that the recombinant protein expressed in BHK cells consisted of three distinct glycoforms differing in heparin affinity (39), the discrepancies between the past and current studies may reflect some heterogeneity in the wild-type and mutant antithrombin preparations employed in the past study. Whereas our studies were done with the purified highest affinity glycoform lacking carbohydrate at Asn135, the past study appears to have been done with a preparation enriched in the dominant glycoform possessing carbohydrate at this site. Interestingly, our results confirm the previous observation that the heparin-binding defect in W49K antithrombin is less when a full-length heparin is



bound than when the pentasaccharide is bound (28). This may be due to the ability of the longer heparin to directly interact with the substituted lysine side chain and decrease the overall binding defect, as was suggested previously.

Similar to the findings with other heparin-binding site mutations in antithrombin, mutation of Trp49 did not affect the ability of heparin to conformationally activate antithrombin as judged from the essentially normal tryptophan fluorescence enhancement produced in W49K antithrombin by heparin. The normalcy of the observed fluorescence enhancement was indicated on the basis of the established contributions of the four tryptophans to the fluorescence of the native and activated conformational states of antithrombin in previous studies (31). W49K antithrombin also showed normal rates of inhibition of thrombin and factor Xa, which were accelerated by heparin to the same extents as the wild-type inhibitor. The mutation thus does not appear to perturb the native and activated conformational states of antithrombin and only the ability of heparin to alter the equilibrium between these states.

The heparin pentasaccharide binding defect in W49K antithrombin was found to be due principally to a loss of nonionic interactions, although the loss of a single ionic interaction additionally contributed to the affinity loss at pH 7.4 but not at pH 6. Decreasing the pH from 7.4 to 6 has been shown to enhance the heparin-binding affinity of wild-type antithrombin by increasing the ionic contribution to the binding (32). The additional ionic interactions made by the pentasaccharide at pH 6 could disfavor nonproductive modes of binding permitted at pH 7.4 by the positively charged lysine substitution. The observed nonionic contribution to the affinity loss may thus more accurately reflect a pH-independent contribution of the Trp49 side chain to the binding of the pentasaccharide.

Rapid kinetic studies showed that the heparin-binding defect in W49K antithrombin minimally involved the initial low-affinity binding of heparin and was largely due to effects on the subsequent heparin-induced conformational activation step. Interestingly, the initial binding step showed a somewhat enhanced affinity for binding the full-length heparin but normal affinity for the pentasaccharide. This suggests that the lysine substitution does have a small positive effect on the initial weak largely electrostatic binding of the longer heparin because of its proximity to negatively charged saccharide residues extending from the reducing end of the pentasaccharide. However, it does not fully explain the reduced binding defect observed with the full-length heparin because the full-length heparin also had a smaller effect than the pentasaccharide on the second conformational activation step. The overriding effect of the W49K mutation on the second conformational activation step involved a modest reduction in the rate constant for conformational activation but a substantial increase in the rate constant for reversal of conformational activation. The major effect of the Trp49 mutation is thus to decrease the stability of the activated conformation, principally by increasing the rate at which the activated conformation reverts back to the native conformation. Comparisons of the effect of the Trp49 mutation with that of other heparin-binding site mutations indicate that Trp49 is less important than the three major heparin contact residues, Lys114, Lys125, and Arg129, which contribute ~50, ~25–33, and ~28–35% of the total binding energy

(17–19). It is also less important than Phe122, which indirectly contributes to heparin binding through nonionic interactions with the stems of the critical basic residues that interact with the pentasaccharide (38). Trp49 nevertheless plays a somewhat greater role than Lys11, Arg13, Arg24, Arg47, and Phe121, which individually contribute 9–18% of the total heparin-binding energy (40–42). However, because Trp49 is not a contact residue, its effect on heparin binding must be indirect, as was previously found for Phe121, Phe122, and Arg24 (40, 42). In fact, the effects of the W49K mutation on heparin binding are remarkably similar to those produced by the mutation of Arg24. Thus, the major effect of the latter mutation was to destabilize the activated antithrombin conformation by increasing the rate of reversal of the conformational activation step (42). This destabilization could be ascribed to a critical role of Arg24 in stabilizing the P helix whose formation in the activated state serves to orient the pivotal Lys114 residue for optimal binding of the pentasaccharide. This stabilization of the P helix was mediated by hydrogen bonds between the N-terminal Arg24 and both Glu113 and Asp117 on the helix.

The effects of the Trp49 to lysine mutation may likewise involve an indirect role of this tryptophan in stabilizing the changes in the secondary structure that accompany conformational activation. A comparison of the structures of free antithrombin in the native conformation and pentasaccharide-bound antithrombin in the activated conformation (Figure 5) suggest that Trp49 may stabilize the conformational changes in the A helix, which are responsible for orienting Arg46 and Arg47 for binding the pentasaccharide. These changes involve a substantial rearrangement of the helix that cause a repositioning of Trp49, Glu50, and Lys53. Notably, the indole ring of Trp49 flips to position Trp49 and Lys53 for a favorable cation– $\pi$  interaction, and Glu50 undergoes a similar flipping of its side chain, which causes the disruption of a salt bridge with Lys53 in the native conformation and establishes a new hydrogen-bonding interaction with Ser112 in the newly formed P helix. The Trp49 structural change is evidenced by a 15 nm blue shift and enhancement of Trp49 fluorescence upon heparin activation of the inhibitor (31), which can be accounted for by the transfer of the hydrogen-bonding nitrogen of the indole ring from a solvent exposed to a buried position after flipping of the ring (43). The replacement of Trp49 with a lysine can thus be expected to abolish the cation– $\pi$  interaction with Lys53 as well as introduce an unfavorable, charge–charge repulsion between these residues in the activated state. These effects could in turn reduce the ability of Glu50 to hydrogen bond with Ser112 and alter the stability of the P helix.

The importance of Trp49, Glu50, Lys53, and Ser112 in heparin activation is supported by the high degree of conservation of these residues in the 13 vertebrate antithrombins that have been sequenced (30). Glu50 is absolutely conserved in all known sequences, whereas residue 49 is Trp and residue 53 is Lys or Arg in all cases except for the frog. In frog antithrombin, residues 49 and 53 are Tyr and Gln, consistent with a hydrogen-bonding interaction replacing the cation– $\pi$  interaction in this activated antithrombin. Ser112 is conserved in all cases except for two species, which have a lysine, but such a replacement would still allow a favorable interaction with Glu50.



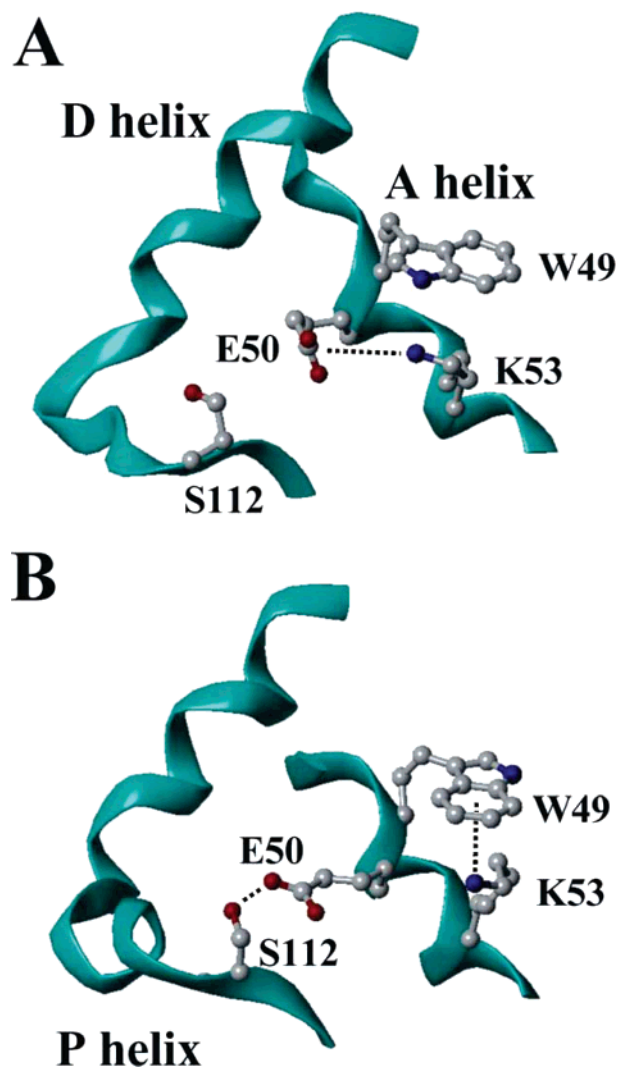


FIGURE 5: Orientation of Trp49, Glu50, Lys53, and Ser112 in the native form (A) and the allosterically activated form (B) of antithrombin. The pentasaccharide-binding site is formed by helices A, D, and P. The structure of pentasaccharide has been omitted in B for clarity. Side chains of Trp49, Glu50, Lys53, and Ser112 are shown in ball-and-stick representation (carbon in gray, nitrogen in blue, and oxygen in red). Flipping of the Trp49 indole ring in the allosteric activation of the serpin facilitates the formation of a W49–K53 cation– $\pi$  interaction and S112–E50 hydrogen bond ( $\cdots$  in B) in the activated state, following a disruption of the K53–E50 salt bridge present in the native state ( $\cdots$  in A). See the text for details.

Because our results indicate that a loss of nonionic interactions is largely responsible for destabilizing the activated conformation of W49K antithrombin, the lysine replacement cannot alter the structure of the activated state in a manner that significantly affects the interactions of basic residues. The major pH-independent effect of the mutation on nonionic interactions implies that unfavorable interactions are likely to be introduced in the activated state by the loss of the cation– $\pi$  interaction between Trp49 and Lys53 and the introduction of an unfavorable, charge–charge repulsion between Lys53 and the substituted lysine in W49K antithrombin. Replacing the Trp49 side chain with other non-aromatic residues would also be expected to disrupt the Trp49–Lys53 cation– $\pi$  interaction without introducing charge–charge repulsion and allow an assessment of the contribution of this apparently highly conserved interaction

in stabilizing the activated conformation of helix A. The conservative replacement of Trp49 with Phe was found to have minimal effects on heparin binding and activation of the inhibitor or on the stability of the protein in a previous study (31), but the Phe replacement would be expected to retain the cation– $\pi$  interaction and account for the minor effects on activation. Further mutagenesis studies will be required to confirm our proposed role of Trp49 in mediating heparin activation of antithrombin.

In conclusion, the Trp49 residue was found to play an important role in heparin activation of antithrombin. Mutation of Trp49 to Lys resulted in substantial losses of ionic and nonionic interactions, while impairing the conformational activation step in the heparin activation process. The impairment could be accounted for by the disruption of a network of interactions involving Trp49, Glu50, and Lys53 of helix A and Ser112 of helix P, which stabilize the activated state of serpin. This work puts forward for the first time this network of interactions, which can be put to test through additional mutagenesis experiments. Although, no natural mutations of Trp49 appear to be known, the magnitude of the binding defect is greater than that of Arg47, of which several natural mutations have been reported and found to predispose individuals to thrombotic conditions (44–47). Therefore, if a nonconservative Trp49 mutation was to occur naturally, one would expect a similar thrombotic phenotype.

## REFERENCES

- Olson, S. T., and Björk, I. (1994) Regulation of thrombin activity by antithrombin and heparin, *Semin. Thromb. Hemostasis* 20, 373–409.
- Björk, I., and Olson, S. T. (1997) Antithrombin. A bloody important serpin, in *Chemistry and Biology of Serpins* (Church, F. C., Cunningham, D. D., Ginsburg, D., Hoffman, M., Stone, S. R., and Tollefsen, D. M., Eds.) pp 17–33, Plenum Press, New York.
- Gettins, P. G. (2002) Serpin structure, mechanism, and function, *Chem. Rev.* 102, 4751–4803.
- Olson, S. T., Björk, I., and Shore, J. D. (1993) Kinetic characterization of heparin-catalyzed and uncatalyzed inhibition of blood coagulation proteinases by antithrombin, *Methods Enzymol.* 222, 525–559.
- Bedsted, T., Swanson, R., Chuang, Y. J., Bock, P. E., Björk, I., and Olson, S. T. (2003) Heparin and calcium ions dramatically enhance antithrombin reactivity with factor IXa by generating new interaction exosites, *Biochemistry* 42, 8143–8152.
- Olson, S. T., Swanson, R., Raub-Segall, E., Bedsted, T., Sadri, M., Petitou, M., Herault, J. P., Herbert, J. M., and Björk, I. Accelerating ability of synthetic oligosaccharides on antithrombin inhibition of proteinases of the clotting and fibrinolytic systems. Comparison with heparin and low-molecular-weight heparin, *Thromb. Haemostasis* 92, 929–939.
- Linhardt, R. J., and Loganathan D. (1990) Heparin, heparinoids and heparin oligosaccharides: Structure and biological activities in *Biomimetic Polymers* (Gebelein, C. G., Ed.) pp 135–173, Plenum Press, New York.
- Rabenstein, D. L. (2002) Heparin and heparan sulfate: Structure and function, *Nat. Prod. Rep.* 19, 312–331.
- Olson, S. T., and Chuang, Y. J. (2002) Heparin activates antithrombin anticoagulant function by generating new interaction sites (exosites) for blood clotting proteinases, *Trends Cardiovasc. Med.* 12, 331–338.
- Langdown, J., Johnson, D. J. D., Baglin, T. P., and Huntington, J. A. (2004) Allosteric activation of antithrombin critically depends upon hinge region extension, *Biochemistry* 279, 47288–47297.
- Olson, S. T., and Shore, J. D. (1982) Demonstration of a two-step reaction mechanism for inhibition of  $\alpha$ -thrombin by antithrombin III and identification of the step affected by heparin, *J. Biol. Chem.* 257, 14891–14895.



12. Danielsson, A., Raub, E., Lindahl, U., and Björk, I. (1986) Role of ternary complexes, in which heparin binds both antithrombin and proteinase, in the acceleration of the reactions between antithrombin and thrombin or factor Xa, *J. Biol. Chem.* 261, 15467–15473.
13. Olson, S. T. (1988) Transient kinetics of heparin-catalyzed protease inactivation by antithrombin III. Linkage of protease–inhibitor–heparin interactions in the reaction with thrombin, *J. Biol. Chem.* 263, 1698–1708.
14. Rezaie, A. R. (1998) Calcium enhances heparin catalysis of the antithrombin–factor Xa reaction by a template mechanism. Evidence that calcium alleviates Gla domain antagonism of heparin binding to factor Xa, *J. Biol. Chem.* 273, 16824–16827.
15. Rezaie, A. R., and Olson, S. T. (2000) Calcium enhances heparin catalysis of the antithrombin–factor Xa reaction by promoting the assembly of an intermediate heparin–antithrombin–factor Xa bridging complex. Demonstration by rapid kinetics studies, *Biochemistry* 39, 12083–12090.
16. Jin, L., Abrahams, J.-P., Skinner, R., Petitou, M., Pike, R. N., and Carrell, R. W. (1997) The anticoagulant activation of antithrombin by heparin, *Proc. Natl. Acad. Sci. U.S.A.* 94, 14683–14688.
17. Desai, U. R., Swanson, R. S., Bock, S. C., Björk, I., and Olson, S. T. (2000) The role of arginine 129 in heparin binding and activation of antithrombin, *J. Biol. Chem.* 275, 18976–18984.
18. Arocas, V., Bock, S. C., Raja, S., Olson, S. T., and Björk, I. (2001) Lysine 114 of antithrombin is of crucial importance for the affinity and kinetics of heparin pentasaccharide binding, *J. Biol. Chem.* 276, 43809–43817.
19. Schedin-Weiss, S., Desai, U. R., Bock, S. C., Gettins, P. G. W., Olson, S. T., and Björk, I. (2002) Importance of Lysine 125 for heparin binding and activation of antithrombin, *Biochemistry* 41, 4779–4788.
20. Arocas, V., Turk, B., Bock, S. C., Olson, S. T., and Björk, I. (2000) The region of antithrombin interacting with full-length heparin chains outside the high-affinity pentasaccharide sequence extends to Lys136 but not to Lys139, *Biochemistry* 39, 8512–8518.
21. Olson, S. T., Björk, I., Sheffer, R., Craig, P. A., Shore, J. D., and Choay, J. (1992) Role of the antithrombin binding pentasaccharide in heparin acceleration of antithrombin–proteinase reactions, *J. Biol. Chem.* 267, 12528–12538.
22. Chang, J. Y., and Tran, T. H. (1986) Antithrombin III Basel. Identification of a Pro–Leu substitution in a hereditary abnormal antithrombin with impaired heparin cofactor activity, *J. Biol. Chem.* 261, 1174–1176.
23. Blackburn, M. N., Smith, R. L., Carson, J., and Sibley, C. C. (1984) The heparin-binding site of antithrombin III. Identification of a critical tryptophan in the amino acid sequence, *J. Biol. Chem.* 259, 939–941.
24. Björk, I., and Nordling, K. (1979) Evidence by chemical modification for the involvement of one or more tryptophanyl residues of bovine antithrombin in the binding of high-affinity heparin, *Eur. J. Biochem.* 102, 497–502.
25. Chowdhury, V., Mille, B., Olds, R. J., Lane, D. A., Watton, J., Barrowcliffe, T. W., Pabinger, I., Woodcock, B. E., and Thein, S. L. (1995) Antithrombins Southport (Leu 99 to Val) and Vienna (Gln 118 to Pro): Two novel antithrombin variants with abnormal heparin binding, *Br. J. Haematol.* 89, 602–609.
26. Okajima, K., Abe, H., Maeda, S., Motomura, M., Tsujihata, M., Nagataki, S., Okabe, H., and Takatsuki, K. (1993) Antithrombin III Nagasaki (Ser116–Pro): A heterozygous variant with defective heparin binding associated with thrombosis, *Blood* 81, 1300–1305.
27. Watton, J., Longstaff, C., Lane, D. A., and Barrowcliffe, T. W. (1993) Heparin binding affinity of normal and genetically modified antithrombin III measured using a monoclonal antibody to the heparin binding site of antithrombin III, *Biochemistry* 32, 7286–7293.
28. Gettins, P., Choay, J., Crews, B. C., and Zettlmeissl, G. (1992) Role of tryptophan 49 in the heparin cofactor activity of human antithrombin III, *J. Biol. Chem.* 267, 21946–21953.
29. Johnson, D. J. D., and Huntington, J. A. (2003) Crystal structure of antithrombin in a heparin-bound intermediate state, *Biochemistry* 42, 8712–8719.
30. Backovic, M., and Gettins, P. G. (2002) Insight into residues critical for antithrombin function from analysis of an expanded database of sequences that includes frog, turtle, and ostrich antithrombins, *J. Proteome Res.* 1, 367–373.
31. Meagher, J. L., Beechem, J. M., Olson, S. T., and Gettins, P. G. (1998) Deconvolution of the fluorescence emission spectrum of human antithrombin and identification of the tryptophan residues that are responsive to heparin binding, *J. Biol. Chem.* 273, 23283–23289.
32. Desai, U. R., Petitou, M., Björk, I., and Olson, S. T. (1998) Mechanism of heparin activation of antithrombin. Role of individual residues of the pentasaccharide activating sequence in the recognition of native and activated states of antithrombin, *J. Biol. Chem.* 273, 7478–7487.
33. Turk, B., Brieditis, I., Bock, S. C., Olson, S. T., and Björk, I. (1997) The oligosaccharide side chain on Asn-135 of  $\alpha$ -antithrombin, absent in  $\beta$ -antithrombin, decreases the heparin affinity of the inhibitor by affecting the heparin-induced conformational change, *Biochemistry* 36, 6682–6691.
34. Olson, S. T., Halvorson, H. R., and Björk, I. (1991) Quantitative characterization of the thrombin–heparin interaction. Discrimination between specific and nonspecific binding models, *J. Biol. Chem.* 266, 6342–6352.
35. Olson, S. T., and Björk, I. (1991) Predominant contribution of surface approximation to the mechanism of heparin acceleration of the antithrombin–thrombin reaction. Elucidation from salt concentration effects, *J. Biol. Chem.* 266, 6353–6364.
36. Mascotti, D. P., and Lohman, T. M. (1995) Thermodynamics of charged oligopeptide–heparin interactions, *Biochemistry* 34, 2908–2915.
37. Olson, S. T., Srinivasan, K. R., Björk, I., and Shore, J. D. (1981) Binding of high affinity heparin to antithrombin III. Stopped flow kinetic studies of the binding interaction, *J. Biol. Chem.* 256, 11073–11079.
38. Manning, G. S. (1978) The molecular theory of polyelectrolyte solutions with applications to the electrostatic properties of polynucleotides, *Q. Rev. Biophys.* 11, 179–249.
39. Fan, B., Crews, B. C., Turko, I. V., Choay, J., Zettlmeissl, G., and Gettins, P. (1993) Heterogeneity of recombinant human antithrombin III expressed in baby hamster kidney cells. Effect of glycosylation differences on heparin binding and structure, *J. Biol. Chem.* 268, 17588–17596.
40. Jairajpuri, M. A., Lu, A., Desai, U. R., Olson, S. T., Björk, I., and Bock, S. C. (2003) Antithrombin III phenylalanines 122 and 121 contribute to its high affinity for heparin and its conformational activation, *J. Biol. Chem.* 278, 15941–15950.
41. Arocas, V., Bock, S. C., Olson, S. T., and Björk, I. (1999) The role of Arg46 and Arg47 of antithrombin in heparin binding, *Biochemistry* 38, 10196–10204.
42. Schedin-Weiss, S., Desai, U. R., Bock, S. C., Olson, S. T., and Björk, I. (2004) Roles of N-terminal region residues Lys11, Arg13, and Arg24 of antithrombin in heparin recognition and in promotion and stabilization of the heparin-induced conformational change, *Biochemistry* 43, 675–683.
43. Lakowicz, J. R. (2000) On spectral relaxation in proteins, *Photochem. Photobiol.* 72, 421–437.
44. Koide, T., Odani, S., Takahashi, K., Ono, T., and Sakuragawa, N. (1984) Antithrombin III Toyama: Replacement of arginine-47 by cysteine in hereditary abnormal antithrombin III that lacks heparin-binding ability, *Proc. Natl. Acad. Sci. U.S.A.* 81, 289–293.
45. Owen, M. C., Borg, J. Y., Soria, C., Soria, J., Caen, J., and Carrell, R. W. (1987) Heparin binding defect in a new antithrombin III variant: Rouen, 47 Arg to His, *Blood* 69, 1275–1279.
46. Borg, J. Y., Owen, M. C., Soria, C., Soria, J., Caen, J., and Carrell, R. W. (1988) Proposed heparin binding site in antithrombin based on arginine 47. A new variant Rouen-II, 47 Arg to Ser, *J. Clin. Invest.* 81, 1292–1296.
47. Wolf, M., Boyer-Neumann, C., Molho-Sabatier, P., Neumann, C., Meyer, D., and Larrieu, M. J. (1990) Familial variant of antithrombin III (AT III Bligny, 47Arg to His) associated with protein C deficiency, *Thromb. Haemostasis* 63, 215–219.

BI0507411